Online Estimation of Battery Parameters and State of Charge Using Continuous Time Domain Identification Method

Cheng Zhang[1], Quang Truong Dinh [1], Walid Allafi[1], James Marco[1], and Jong Il Yoon[2*]
[1] WMG, University of Warwick, Coventry, UK
[2]Korea Construction Equipment Technology Institute, Gunsan 573-540 Sandan-ro 36, Korea
[*]Corresponding: jiyoon@koceti.re.kr

Abstract – **Battery equivalent circuit models (ECMs) are widely used in battery management systems (BMSs), such as in electric vehicles (EVs). The battery terminal voltage-current (VI) dynamics and the ECM parameters depend on the operating conditions, such as the state of charge (SOC) and temperature. Online parameter estimation can improve not only the modelling accuracy, but also the performance of model-based SOC estimation, which plays a key role in BMS. This paper presents a continuous-time (CT) domain algorithm for online co-estimation of the battery ECM parameters and SOC, using the linear integral filter (LIF) method. Compared with the conventional discrete time domain least square algorithm, the proposed CT LIF technique has superior performance at capturing the battery slow dynamics, which can further improve the SOC estimation accuracy. Experimental data are collected using a Li ion battery (LIB), and the results are analyzed to verify the efficacy of the proposed algorithm.**

Keywords - equivalent circuit model, recursive parameter and SOC estimation, linear integral filter.

1 INTRODUCTION

Equivalent circuit models (ECMs) have been widely used in battery management systems of battery energy storage systems due to the ease of parametrization and implementation and acceptable modelling accuracy. An ECM uses a combination of electric components, including resistors and capacitors, to represent the battery terminal voltage-current (VI) behavior. Figure 1 presents a typical ECM, where v,i are the battery terminal voltage and current, respectively. The battery open circuit voltage (OCV) depends on the battery state of charge (SOC). The R_0 stands for the battery series resistance, and the RC networks are used to capture the dynamics voltage relaxation effects.

One key issue with ECM is that the model parameters depend on the operating conditions, for instance, the ambient temperature, SOC and state of health (SOH). For example, a Li ion battery (LIB) cell shows nearly doubled internal resistance as the temperature drops from 25 $^{\circ}C$ to 0 $^{\circ}C$ [1]. The parameter dependency can be described using a look-up table trained offline. However, this offline battery characterization is time-consuming. Moreover, the tabulated ECM parameters will lose efficacy as the battery degrades. Therefore, online recursive parameter identification schemes should be used to keep track of the evolving ECM parameters to improve modelling accuracy.

SOC estimation is another key issue in BMSs [2]. Existing SOC estimation algorithms based on onboard VI measurements include Ampere hour (Ah) counting and OCV-based algorithms [1, 2]. ECM-based state observer techniques, such as Kalman filter (KF), unscented KF (UKF), H-infinite filter, etc. [3-6], have been widely used for real-time battery SOC estimation by combining the advantages of the Ah and OCV-based methods. The SOC estimation performance depends on the model accuracy, and therefore online estimation of the ECM parameters can improve not only the modelling accuracy, but also the SOC estimation performance [7].

Various of recursive identification algorithms have been proposed for online ECM parameter estimation, such as the recursive least square (RLS) schemes [1, 8] and the state-observer based algorithms including KF, UKF [3, 4], H-infinite filter [9], etc. For example, Plett suggested joint/dual extended KF and UKF for co-estimation of the ECM parameters, SOC and SOH [3, 4]. Chen et al [5] proposed using dual H-infinite filters for simultaneous estimation of model parameters and SOC. A combination of the RLS algorithm for recursive parameter identification and the KF algorithm for SOC estimation has been reported in [10]. These algorithms are generally derived and implemented in discrete-time (DT) domain. However, for the battery system consisting of both fast and slow dynamics (e.g., the charge transfer as the fast dynamics and diffusion as the slow dynamics), the time constants of the RC branches in Figure 1 will be widely separated. This poses severe numerical problems to the DT domain identification methods like RLS. Another problem shows in the case of fast sampling because the model poles will lie close to the unit circle in the complex domain, so that the model parameters are more poorly defined in statistical terms [11]. These problems can be addressed using continuous time (CT) domain identification algorithms. The advantages of CT domain identification algorithms compared to the DT methods include (i) that the model parameters are independent of the sampling time and, (ii) that the CT methods can deal with widely separated system poles. Xia et al [12] compared the CT and DT algorithms, for ECM parameter optimization, and concluded that the CT method has superior performance for identifying a stiff system like the battery, especially in

the presence of measurement noises and with low data storage resolution. One limitation is that the proposed algorithm is implemented offline, and thus cannot be used for online recursive estimation of ECM parameters and SOC.

This paper presents a CT domain identification method for online co-estimation of the battery parameters and SOC. The linear integral filter (LIF) algorithm is adopted for the ECM parameter estimation. Comparing with the DT LS method, the LIF algorithm shows improved modelling accuracy, which further leads to improved SOC estimation performance. The proposed algorithm can be implemented offline or recursively for realtime applications. Test data are collected on a LIB cell and the experimental results verify the superiority of the CT LIF algorithm over the DT RLS method.

2 Battery ECM

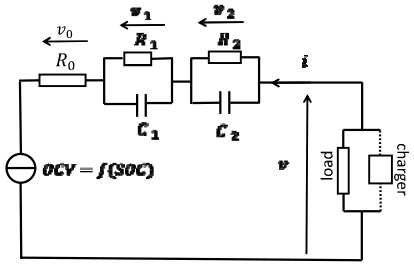

Figure 1 Battery equivalent circuit model

2.1 DT RLS

The battery ECM is depicted in Figure 1, the symbols $OCV, v, i, R_0, R_1C_1, R_2C_2$ have been explained in the Introduction section. Assume that zero-order holder is applied for the VI measurements, the RC dynamics can then be put as

$$v_j(k+1) = a_{j,d}v_j(k) + b_{j,d}i(k), \quad j = 1,2 \qquad (1)$$

where

$$a_{j,d} = exp(-T_s / R_j / C_j)$$
$$b_{j,d} = R_j(1-a_{j,d})$$

Where $v_j(k)$ stands for $v_j(kT_s)$, and T_s is the sampling interval in seconds.

Let z be the time shift operator, i.e., $zx(k) = x(k+1)$. Eq (1) can be re-written as

$$v_j(k) = \frac{b_{j,d}}{z - a_{j,d}} i(k)$$

The Ah method is used for calculating the battery SOC [1], i.e.,

$$SOC(k+1) = SOC(k) + \frac{Ts}{C_n} i(k) \qquad (2)$$

where C_n is the battery nominal capacity.

The model terminal voltage in Figure 1 is a sum of the OCV and the over-potentials as follows,

$$v(k) = OCV(k) + v_0(k) + v_1(k) + v_2(k) \qquad (3)$$

Let $v_s = v_0 + v_1 + v_2 = v - OCV$. In case of unknown battery SOC and OCV, an estimated OCV value can be used, i.e.,

$$v_s = v - \overline{OCV} = v - f(\overline{SOC}) \qquad (4)$$

where $\overline{OCV}$ and $\overline{SOC}$ are the OCV and SOC estimations, respectively.

Combining Eq (3) and Eq (4) leads to,

$$v_s = v_0 + v_1 + v_2 + (OCV - \overline{OCV}) \qquad (5)$$

Define

$$c_0 = OCV - \overline{OCV} = f(SOC) - f(\overline{SOC}) \approx k_s(SOC - \overline{SOC}),$$

which depends on the SOC error $SOC - \overline{SOC}$ and the slope of the OCV-SOC curve k_s. For the LIB cell used in this paper having a quasi-linear OCV-SOC curve as depicted in Figure 5, the slope k_s can be taken as a constant or a slowing varying variable. On the other hand, the SOC error $SOC - \overline{SOC}$ is a constant if both SOC and $\overline{SOC}$ are updated using Eq (2). Therefore c_0 can be taken approximately as a constant. Eq (5) leads to

$$\begin{aligned} v_s(k) &= v_0(k) + v_1(k) + v_2(k) + c_0 \\ &= (R_0 + \frac{b_{1,d}}{z - a_{1,d}} + \frac{b_{2,d}}{z - a_{2,d}})i(k) + c_0 \\ &= \frac{\theta_{d,4}z^2 + \theta_{d,3}z + \theta_{d,2}}{z^2 - \theta_{d,1}z - \theta_{d,0}} i(k) + c_0 \end{aligned} \qquad (6)$$

The relationship between θ_d and the RC values is straightforward and thus omitted here. Eq (6) can be reformulated into the linear in the parameter (LITP) way as follows

$$\begin{aligned} z^2 v_s(k) &= \theta_{d,1} z v_s(k) + \theta_{d,0} v_s(k) + \theta_{d,4} z^2 i(k) \\ &+ \theta_{d,3} z i(k) + \theta_{d,2} i(k) + (1 - \theta_{d,1} - \theta_{d,0}) c_0 \end{aligned} \qquad (7)$$

Let

$$y_d(k) = z^2 v_s(k),$$
$$\theta_d = \left[\theta_{d,1}, \theta_{d,0}, \theta_{d,4}, \theta_{d,3}, \theta_{d,2}, (1-\theta_{d,1}-\theta_{d,0})c_0\right]^T,$$
$$\varphi_d(k) = \left[zv_s(k), v_s(k), z^2 i(k), zi(k), i(k), 1\right]^T$$

Eq (7) yields

$$y_d(k) = \theta_d^T \varphi_d(k) \quad (8)$$

The parameters θ_d can be optimized using the LS algorithm or recursively using RLS in Eq (9).

Problem Formulation:

$$y(k) = \theta^T \varphi(k)$$

RLS solution

$$e(k+1) = y(k+1) - \varphi^T(k+1)\theta(t)$$
$$\theta(k+1) = \theta(k) + P(k+1)\varphi(k+1)e(k+1)$$
$$P(k+1) = P(k) - \frac{P(k)\varphi(k+1)\varphi^T(k+1)P(k)}{1+\varphi^T(k+1)P(k)\varphi(k+1)} + Q_0 \quad (9)$$

The initial parameters $\theta(0), P(0)$ can be obtained by performing a block-wise LS identification procedure as discussed within [13]. Q_0 is set to be $P(0)/1000$ in this paper.

2.2 CT LIT method

The CT domain dynamics of a RC network can be expressed as

$$\frac{d}{dt}v_j(t) = -a_{j,c}v_j(t) + b_{j,c}i(t), j = 1,2 \quad (10)$$

Where $a_{j,c} = 1/R_j/C_j, b_{j,c} = 1/C_j$.

Eq (10) leads to $v_j = \frac{b_{j,c}}{s+a_{j,c}}i$, where s represents the Laplace operator.

Similar to Eq (6), the sum of over-potentials v_s can be calculated as follows,

$$\begin{aligned} v_s(t) &= v_0(t) + v_1(t) + v_2(t) + c_0 \\ &= (R_0 + \frac{b_{1,c}}{s+a_{1,c}} + \frac{b_{2,c}}{s+a_{2,c}})i(t) + c_0 \\ &= \frac{\theta_{c,4}s^2 + \theta_{c,3}s + \theta_{c,2}}{s^2 + \theta_{c,1}s + \theta_{c,0}}i(t) + c_0 \end{aligned} \quad (11)$$

Next, the LITP form of Eq (11) is given below,

$$\begin{aligned} &v_s^{(2)}(t) = -\theta_{c,1}v_s^{(1)}(t) - \theta_{c,0}v_s(t) + \theta_{c,4}i^{(2)}(t) \\ &+\theta_{c,3}i^{(2)}(t) + \theta_{c,2}i(t) + c_0\theta_{c,0} \end{aligned} \quad (12)$$

Where $x^{(k)}$ stands for the k-th order derivative of x. The derivative terms $v_s^{(k)}(t), i^{(k)}(t)$ are not directly measurable. Different algorithms can be used to deal with these derivative terms, such as the state variable filter, LIF, and modulating function methods, etc. The LIF method is adopted in this paper because of its ease of digital implementation and the relief of calculating initial conditions.

Perform two successive integral calculations on both sides of Eq (12), i.e.,

$$\int_{t_2-LT_s}^{t_2}\int_{t_1-LT_s}^{t_1} \text{Eq (12)} dt dt_1 \quad (13)$$

Where L is a positive integer and LT_s is the length of the integral window.

Let

$$f_0 = (0.5 + z^{-1} + z^{-2} + ... + z^{-L+1} + 0.5z^{-L})T_2$$
$$f_1 = 1 - z^{-L}$$

Then, Eq (13) can be re-expressed as

$$\begin{aligned} &f_1^2 v_s(t) = -\theta_{c,1}f_0 f_1 v_s(t) - \theta_{c,0}f_0^2 v_s(t) + \theta_{c,4}f_1^2 i(t) \\ &+\theta_{c,3}f_0 f_1 i(t) + \theta_{c,2}f_0^2 i(t) + c_0\theta_{c,0}(LT_s)^2 \end{aligned} \quad (14)$$

Define

$$y_c(t) = f_1^2 v_s(t)$$
$$\theta_c = [-\theta_{c,1}, -\theta_{c,0}, \theta_{c,4}, \theta_{c,3}, \theta_{c,2}, c_0\theta_{c,0}(LT_s)^2]^T$$
$$\varphi_c = [f_0 f_1 v_s(t), f_0^2 v_s(t), f_1^2 i(t), f_0 f_1 i(t), f_0^2 i(t), 1]^T$$

Eq (14) leads to

$$y_c(t) = \theta_c^T \varphi_c(t) \quad (15)$$

Eq (15) is a LITP problem and thus the LS and RLS algorithms can be adopted for offline and online parameter estimation.

2.3 SOC Estimation

Since $c_0(k) = OCV(k) - \overline{OCV}(k)$, the estimation of the battery OCV and SOC can be corrected after obtaining c_0 as follows,

$$\begin{aligned} \overline{OCV}_{correction} &= \overline{OCV}(k) + c_{correction} \\ \overline{SOC}_{correction} &= f^{-1}(\overline{OCV}_{correction}) \end{aligned} \quad (16)$$

where f^{-1} stands for SOC-OCV relationship, and

$$c_{correction} = \frac{1}{N_1}\sum_{l=1}^{N_1} c_0(k-l+1)$$

As discussed within [14], there is no need to correct the SOC estimation at every sample, since the convergence of parameter estimation takes certain time. Executing Eq (16) every N_1 samples can avoid unnecessary parameter fluctuations. The estimated

values of OCV, v_s, c_0 will be affected by this SOC correction. Therefore, update these variable as follows,

$$\overline{OCV}(t-2LT_s:t) = \overline{OCV}(t-2LT_s:t) + c_{correction}$$
$$v_s(t-2LT_s:t) = v_s(t-2LT_s:t) - c_{correction}$$
$$c_0(k) = c_0(k) - c_{correction} \quad \text{in } \theta_c \text{ and } \theta_d$$

and the rest model parameters R_0, a_j, b_j will remain unaffected [14]. Note that the Matlab syntax is used here to indicate the way of variable update.

The recursive implementation of the CT LIF algorithm (similarly, the DT RLS scheme) for co-estimation of the ECM parameters and SOC is illustrated in Figure 2.

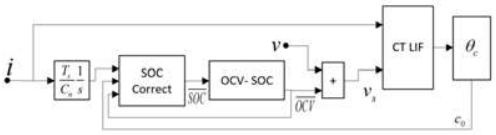

Figure 2 The implementation procedure of the CT LIF algorithm. The Ah method is represented by the integral block, and the 'SOC Correct' block stands for the SOC correction scheme detailed in Section 2.3

3 Experimental Setup

Experimental data have been collected using a commercial cylindrical 3Ah 18650-type cell which comprises graphite negative electrode and a $LiNiCoAlO_2$ positive electrode. A Bitrode battery cycler is used with a thermal chamber for maintaining the ambient temperature constant at 25^oC. First, the battery is fully charged by the constant-current, -constant-voltage (CC-CV) method, and then discharged at 1C rate to 50% SOC, followed by a rest period for two hours. Next, a drive cycle test is applied that reduces the battery SOC to 45% SOC. The VI measurements are plotted in Figure 3. The sampling interval is 1 second.

Another drive cycle test is implemented in a similar way, starting from 75% SOC until end of discharge i.e., when the voltage reaches the cut-off voltage level. Figure 4 depicts the VI measurements.

The battery OCV-SOC relationship is characterized experimentally, as presented in Figure 5.

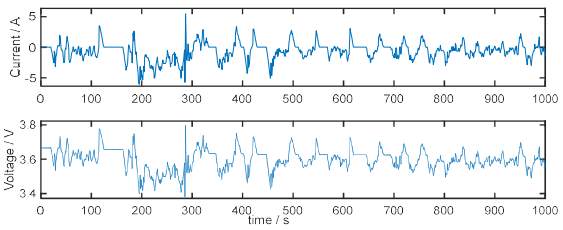

Figure 3 Battery drive-cycle test 1 at 25^oC. The test starts at 50% SOC and ends at 45% SOC

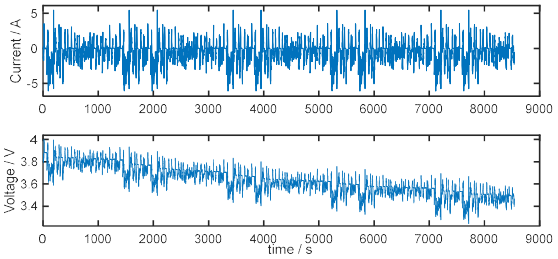

Figure 4 Battery drive-cycle test 2 at 25^oC. The test starts at 75% SOC and ends at end of discharge

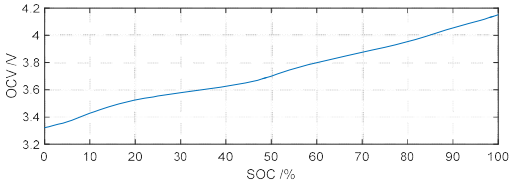

Figure 5 Battery OCV versus SOC

4 Experimental Results

4.1 Offline Model Training

The test data in Figure 3 are used here to train the ECM offline. The battery SOC is assumed to be known and thus the OCV can be calculated using the OCV-SOC relationship in Figure 5. The over-potential v_s can then be obtained, i.e., $v_s = v - OCV$.

The DT LS and CT LIF algorithms are applied for the ECM parameter identification for comparison. Note that $c_0 = 0$ in both cases, since the battery SOC and OCV are known exactly.

The identified model parameters are given as follows,

$$\begin{aligned} &\text{DT LS: } \tau_1 = 1.28s,\ R_1 = 0.93m\Omega, \\ &\tau_2 = 39.4s,\ R_2 = 23.2m\Omega,\ R_0 = 37.7m\Omega \\ &\text{CT LIF: } \tau_1 = 13.2s,\ R_1 = 9.41m\Omega, \\ &\tau_2 = 265s,\ R_2 = 27.4m\Omega,\ R_0 = 37.8m\Omega \end{aligned} \tag{17}$$

The parameter identification results show that the CT model covers a wider time scale, as the larger time constant of the CT model is $\tau_2 = 265s$, compared to $\tau_2 = 39.4s$ of the DT model. The model fitting results are depicted in Figure 6, and it shows that the CT model has superior accuracy. The modelling root mean square errors (RMSEs) are in turn 3.4mV and 7.4mV.

Figure 6 compares the true v_s (i.e., v minuses the true OCV) and the model output v_s (i.e., $v_0 + v_1 + v_2$. v_1, v_2 are calculated using Eq (1)) of the two

comparative algorithms. Based on the parameter identification results in Eq (17) and the modelling error in Figure 6, the higher accuracy of the CT model can be attributed to the wider time scale it covers compared to the DT model. Another distinctive feature in Figure 6 which can support this conclusion is that the DT model shows remarkably larger errors during 200-300s, where the load current is dominated by low frequency components (i.e., <0.01 Hz), indicating that the DT model has a poor fitting at this low frequency range.

Moreover, in case of unknown battery SOC, the battery OCV can only be estimated by $v - v_s$. Therefore, a better v_s estimation accuracy will lead to a better OCV estimation, and thus higher SOC estimation performance.

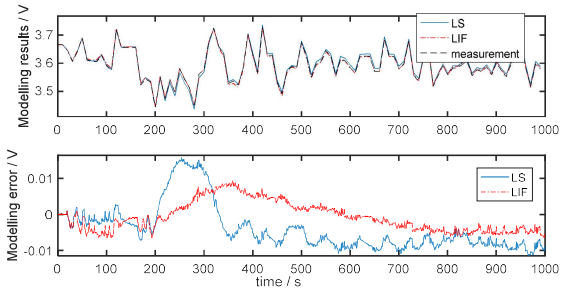

Figure 6 The offline model training results

4.2 Recursive ECM Parameter and SOC Estimation

The test data in Figure 4 are used for recursive ECM parameter and SOC estimation. The SOC range is limited to 75-25% in order to avoid the low SOC level where the battery shows strong nonlinearities. The initial SOC estimation is set to be 65%, with a 10% initial error.

The model parameter identification results are shown in Figure 7. The results show that (i) the CT model covers a larger time scale compared with the DT model. Based on the conclusion in Section 4.1, we can reasonably assume that the CT model will have better performance at capturing the battery slow dynamics; and (ii) the total resistance $R_0 + R_1 + R_2$ using the CT algorithm is higher than that of the DT method. This may be explained by that the DT model cannot capture the battery slow-dynamic resistance (because $\tau_2 < 30s$ in the DT model); and (iii) the R_0 values of the two algorithms are similar, which indicates that both the DT and CT algorithms can reliably estimate this series resistance R_0 ; and (iv) the total resistance shows relatively lower value around 5000 seconds, at about 50% SOC, which indicates that the total resistance of this cell is lower around 50% SOC.

The SOC estimation results are shown in Figure 8. It can be observed that the CT LIF algorithm outperforms the DT LS method in terms of SOC estimation accuracy. The SOC RMSEs are 1.78% and 3.49%, respectively. This different SOC estimation performance can be explained by the v_s estimation results depicted in Figure 9. Since the CT model can capture the battery dynamics within a wider time scale, the v_s estimation error using the LIF algorithm is lower than that of the DT LS method. This higher v_s fitting performance further led to the higher SOC accuracy.

The modelling errors are shown in Figure 10. Note that the modeling errors are different from the v_s estimation errors in Figure 9, because the OCV estimations are different for the two algorithms. Although the DT model shows slightly higher modelling accuracy compared with the CT model (the RMSEs are 4.9mV and 6.0mV in turn.), it comes at an expense of higher SOC estimation error because the DT model cannot capture the slow dynamics within the battery over-potential voltage.

5 Conclusion

This paper proposed using the CT LIF algorithm for recursive co-estimation of the battery ECM parameters and SOC. Compared with the DT LS algorithm, the proposed CT LIF algorithm has superior performance at capturing the battery slow dynamics, which further leads to better SOC estimation accuracy. Test data are collected using a LIB cell, and the experimental results are analyzed to demonstrate the efficacy of the proposed algorithm. The proposed CT LIF algorithm has low computational complexity, and depends only on the online-available VI measurements. Therefore, it has high capability to be implemented for onboard systems to improve the modelling and SOC estimation accuracy.

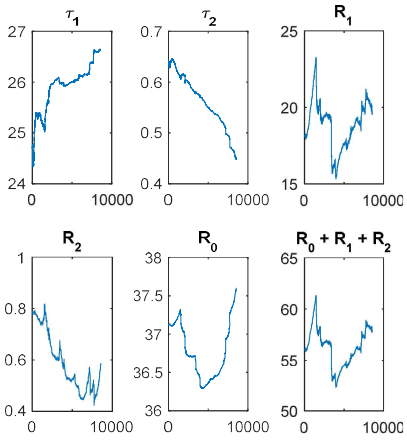

(a)

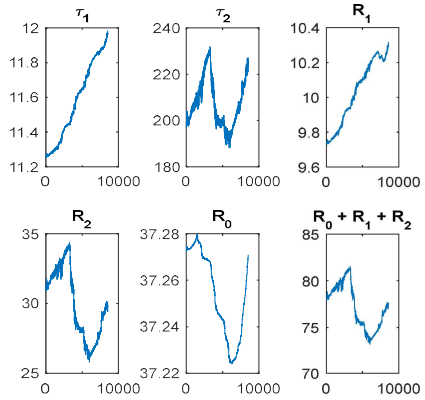

(b)

Figure 7 The parameter identification results using the DT LS method (a) and the CT LIF method (b). The unit for time constants τ is second, and the unit for resistors is $m\Omega$. The x-axes show the time in seconds.

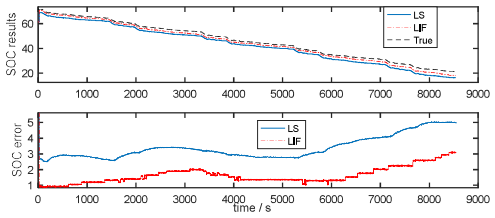

Figure 8 SOC estimation results

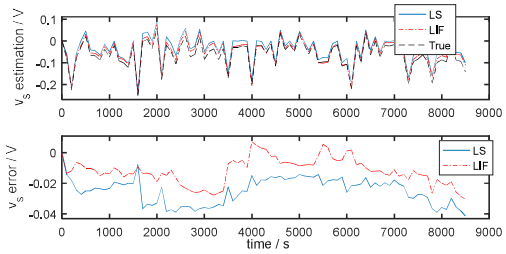

Figure 9 v_s estimation results

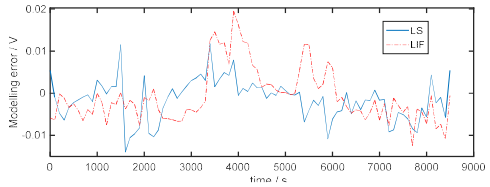

Figure 10 Modelling error

ACKNOWLEDGEMENT

This research was supported by Innovate UK through the Agile Power Management Systems for Marine Vessels, Project Number: 102437 in collaboration with the WMG Centre High Value Manufacturing (HVM), Babcock and Potenza; and was financially supported by the "Next-generation construction machinery component specialization complex development program (R0006266)" through the Ministry of Trade, Industry and Energy(MOTIE) and Korea Institute for Advancement of Technology (KIAT).

REFERENCES

[1] Zhang C, Li K, Pei L, Zhu C. An integrated approach for real-time model-based state-of-charge estimation of lithium-ion batteries. Journal of Power Sources. 2015;283:24-36.
[2] Lu L, Han X, Li J, Hua J, Ouyang M. A review on the key issues for lithium-ion battery management in electric vehicles. Journal of power sources. 2013;226:272-88.
[3] Plett GL. Extended Kalman filtering for battery management systems of LiPB-based HEV battery packs: Part 3. State and parameter estimation. Journal of Power sources. 2004;134(2):277-92
[4] Plett GL. Sigma-point Kalman filtering for battery management systems of LiPB-based HEV battery packs: Part 2: Simultaneous state and parameter estimation. Journal of power sources. 2006;161(2):1369-84
[5] Chen C, Sun F, Xiong R, He H. A Novel Dual H Infinity Filters Based Battery Parameter and State Estimation Approach for Electric Vehicles Application. Energy Procedia. 2016;103:375-80.
[6] Zhang C, Wang LY, Li X, Chen W, Yin GG, Jiang J. Robust and Adaptive Estimation of State of Charge for Lithium-Ion Batteries. IEEE Transactions on Industrial Electronics. 2015;62(8):4948-57.
[7] Hu X, Li S, Peng H, Sun F. Robustness analysis of State-of-Charge estimation methods for two types of Li-ion batteries. Journal of Power Sources. 2012;217:209-19.
[8] Guo X, Kang L, Yao Y, Huang Z, Li W. Joint Estimation of the Electric Vehicle Power Battery State of Charge Based on the Least Squares Method and the Kalman Filter Algorithm. Energies. 2016;9(2):100.
[9] Xiong R, Yu Q, Wang LY, Lin C. A novel method to obtain the open circuit voltage for the state of charge of lithium ion batteries in electric vehicles by using H infinity filter. Applied Energy. 2017.
[10] Wei Z, Zhao J, Ji D, Tseng KJ. A multi-timescale estimator for battery state of charge and capacity dual estimation based on an online identified model. Applied Energy. 2017.
[11] Garnier H, Young P. Time-domain approaches to continuous-time model identification of dynamical systems from sampled data. vol. 1. p. 667-72.
[12] Xia B, Zhao X, De Callafon R, Garnier H, Nguyen T, Mi C. Accurate Lithium-ion battery parameter estimation with continuous-time system identification methods. Applied Energy. 2016;179:426-36.
[13] Ljung L, Söderström T. Theory and practice of recursive identification: JSTOR, 1983.
[14] Zhang C, Marco J, Allafi W, Dinh T, Widanage WD. Online battery electric circuit model estimation on continuous-time domain using linear integral filter method. Proceedings of the World Academy of Science, Engineering and Technology. 2017;4(3):823